1-1-2013

Tidal Variability of Waves and Currents on a Caribbean Barrier Reef

Chelsea Wegner
University of South Carolina

TIDAL VARIABILITY OF WAVES AND CURRENTS ON A CARIBBEAN BARRIER REEF

by

Chelsea Wegner

Bachelor of Science
University of Mary Washington, 2010

Submitted in Partial Fulfillment of the Requirements

For the Degree of Masters of Science in

Marine Science

College of Arts and Sciences

University of South Carolina

2013

Accepted by:

Jean Ellis, Major Professor

James Pinckney, Committee Member

Raymond Torres, Committee Member

Lacy Ford, Vice Provost and Dean of Graduate Studies

ACKNOWLEDGEMENTS

I would like to acknowledge my advisor, Dr. Jean Ellis, and my committee members, Dr. Ray Torres and Dr. Jay Pinckney for their support on this project. I would like to acknowledge Zandy Hillis-Star and Ian Lundgren at Buck Island Reef National Monument (National Park Service) for logistical and field support. Additionally, thank you to Dr. Ben Kisila at the University of Mary Washington for instrument support, Chris Gotschalk and Libe Washburn at the University of California Santa Barbara for the use of their equipment and technical support. I would also like to thank the Department of Geography and the Marine Science Program for funding support.

ABSTRACT

The modern framework of Caribbean coral reefs is a product of resilient structures that have survived extreme variations in sea level for the past 18,000 years. However, the added influences of anthropogenic pressures, including ocean acidification, overfishing, pollution and bleaching make the future response to sea level rise uncertain. Carbonate production in the Caribbean is no longer at these historic rates and reefs may not be able to keep pace with the projected increases in sea level. This could have dramatic impacts on the hydrodynamics in coral reef environments, as reef morphology strongly influences these processes. Coral reefs are regarded as natural breakwaters and in turn, act as shoreline protective structures. If a reef is not at a sufficient height in comparison to the water level, wave energy dissipation is diminished and more energy is transferred to the shoreline, resulting in increased shoreline erosion. Wave driven flows are important in reef environments and it should be expected to see resultant changes in flow associated with various energy regimes, altering lagoonal flushing, water quality and nutrient uptake.

This study was conducted on the southeastern side of Buck Island Reef National Monument, a microtidal *Acropora palmata*-dominated barrier reef system located 2 km NE of St. Croix, USVI. Tidal variability in energy dissipation and current velocities was used to represent future sea level conditions assuming a static reef system. Using Wave Height Pressure Sensors (WHPS) to measure water surface fluctuations, results show that wave energy dissipation is tidally dependent with approximately 20% less dissipation at

higher tides. Using Aquadopp current profilers (ACP), the magnitude of lagoon currents and flushing appear to be wave driven and tidally dependent, with current velocities ranging from 35 cm s^{-1} at low tide and 15 cm s^{-1} at high tide. High tide conditions could be representative of a low tide scenario at an increased sea level of 0.4 m, which is within the range of the 2100 IPCC AR4 projections. Accordingly, the results of this study suggest that sea level rise will have substantial impacts to the hydrodynamics of reef systems, sediment transport processes and coral community structures.

TABLE OF CONTENTS

ACKNOWLEDGEMENTS iii

ABSTRACT iv

LIST OF TABLES vii

LIST OF FIGURES viii

CHAPTER 1: INTRODUCTION 1

CHAPTER 2: METHODS 7

2.1 STUDY SITE 7

2.2 FIELD METHODS 9

2.3 DATA ANALYSIS 14

CHAPTER 3: RESULTS 18

3.1 WAVES 18

3.2 CURRENTS 29

CHAPTER 4: DISCUSSION 35

4.1 IMPACT OF WAVES 35

4.2 IMPACT OF CURRENTS 38

4.3 CONCLUSION 41

REFERENCES 42

LIST OF TABLES

Table 1 Summary of high tide wave parameters 27

Table 2 Summary of low tide wave parameters.....28

Table 3 Surface currents by tidal segment.....32

Table 4 Depth-integrated currents by tidal segment.....33

LIST OF FIGURES

Figure 1 Map of St. Croix 6

Figure 2 Bathymetry of Buck Island Reef National Monument 8

Figure 3 Benthic Habitats 11

Figure 4 Percent Live Coral Cover 12

Figure 5 Instrument Transect Profile 13

Figure 6 Tidal Segments 15

Figure 7 Offshore Forcing Conditions 19

Figure 8 Spectral Density High Tide 22

Figure 9 Spectral Density Low Tide 23

Figure 10 Significant Wave Heights by Location 24

Figure 11 Wave Height versus Water Depth 25

Figure 12 Wave Energy Reduction 26

Figure 13 Surface Currents 30

Figure 14 Net Depth-Integrated Currents 31

Figure 15 ACP2 Net Surface Current vs Water Depth 34

Figure 16 Wave Energy and Coral Diversity 40

CHAPTER 1

INTRODUCTION

Coral reefs are considered natural breakwaters that protect their coincident shorelines. The reef forces wave transformation and breaking (Lugo-Fernandez *et al*. 1998a; Young 1989; Huang *et al.* 2012; Taebi *et al.* 2012) which influences energy dissipation, wave driven flows, bed shear stresses and boundary layer conditions (Young, 1989). Energy dissipation by coral reefs is important for reef morphology, shoreline stability, species distribution and nutrient uptake (Hearn 1999, Huang *et al.* 2012). Reefs are especially important during storm events, forcing large storm waves to break further offshore and preventing or minimizing the shoreline erosion that is often associated with hurricanes and tropical storms (Hubbard *et al.* 1991, Richmond 1993). From an engineering perspective, the height of a breakwater compared to the water depth is crucial in terms of creating an effective structure (Komar 2007). Coral reefs operate under this same principle. The height and slope of the reef and the mean sea level (MSL) determine the degree of energy dissipation that will occur (Hearn 1999).

In a recent study by Storlazzi *et al.* (2011), numerical models were used to demonstrate the impact of future rising sea levels on fringing reefs regarding hydrodynamics and sediment transport. These numerical models suggested a decrease in breaking wave heights at the reef crest, a landward migration of the maximum breaking

wave, greater wave heights and more energetic waves over the reef flat, and an increase in wave induced shear stress on the bed and stronger currents generated as a result of a reduced height in hydrodynamic roughness with greater wave driven flows. Storlazzi *et al.* (2011) also demonstrated that with increasing sea levels, currents would be impacted leading to ecological implications such as a reduction in lagoon flushing and water renewal. These reductions have impacts on nutrient availability, water clarity and community distribution (Roberts *et al.* 1975, Lugo-Fernandez *et al.* 1998, Hearn 1999, Storlazzi *et al.* 2011).

A tidally dependent reduction in energy dissipation has been observed in other reef environments (Roberts and Suhayda 1983; Lugo-Fernandez *et al*. 1998, 1998a). Additionally, wave breaking has been shown to strongly influences currents and circulation within reef lagoons (Roberts and Suhayda 1983; Roberts *et al.* 1975; Lugo-Fernandez *et al.* 1998a, Hearn 1999). Roberts and Suhayda (1983) observed an increase in mean current velocities from 0.07 m s^{-1} at high tide to 0.17 m s^{-1} at low tide at a reef lagoon in Nicaragua. Lugo-Fernandez *et al.* (1998a) also observed stronger currents at low tide because of increased wave breaking. Hearn (1999) explains that the wave breaking at the forereef creates wave setup on the front of the reef flat that creates a pressure gradient over the reef flat and lagoon, which drives the lagoon circulation current. The current strength depends on the degree of wave setup, water depth and friction. The greatest overtopping of water over the reef crest was at low tide, i.e. lower sea levels, which allowed for lagoon water renewal, nutrient transport, temperature and salinity moderation and sediment distribution (Roberts *et al.* 1975; Lugo-Fernandez *et al.*

1998a). These observations emphasize the importance of wave action in the overall health of a reef environment.

The Intergovernmental Panel on Climate Change (IPCC) fourth assessment report (2007) projects a sea level rise of between 0.18 and 0.59 m by 2100. However, other studies suggest that sea level rise may exceed these predications upwards of 1 m (Brown *et al.* 2013). Current sea level trends in St. Croix are approximately 1.74 mm/yr (NOAA 2013) and average cotemporary reef accretion in shallow water habitats in the Caribbean is approximately 0.68 mm yr^{-1} (Perry *et al.* 2013). Therefore, it is important to start assessing how reef processes will change if sea level rise surpasses the rate of vertical reef accretion, which the current trends suggest.

Coral reefs have historically adapted to changes in sea level. Throughout the Holocene and Pleistocene, sea level rose rapidly to levels 100 m higher than present including meltwater pulses that increased rapidly over a short timespan (Macintyre, 2007). Cores can be used to reconstruct how corals responded during these 18,000 years of sea level fluctuations. Neumann and Macintyre (1983) coined the terminology of "keep up", "catch up" and "give up" reefs. The "keep up" reefs maintained growth under conditions of rapid sea level rise, including increased turbidity and sedimentation. However, some reefs ("catch up") lagged in growth, followed by rapid accretion, with fast growing branching coral species. "Give up" reefs were not able to maintain growth rates comparable to the rising sea level and drowned. Many of these "keep up" reefs developed the platform for modern reefs. In addition to sea level rise, modern day reefs face a combination of stressors that Holocene reefs did not (Tager *et al.* 2010), including ocean acidification, pollution, overfishing and bleaching associated with increasing sea

surface temperatures. It is probable that the fate of modern reefs will be different than those of the Holocene with fewer "keep up" reefs.

Perry *et al.* (2013) compared Mid-Holocene and contemporary carbonate production rates and the health of Caribbean reef systems. They found that in shallow water habitats (< 5 m) carbonate production (i.e. accretion) rates were a magnitude lower than Holocene rates, with 0.68 kg $CaCO_3$ yr^{-1} versus 3.6 kg $CaCO_3$ yr^{-1}. A carbonate production of less than 1 kg $CaCO_3$ yr^{-1} is on the threshold of becoming net negative. Additionally taking the moderate (5-10 m) and deep (>10 m) habitats in to consideration, modern rates are 50% lower than mean Holocene rates. Of all of the reefs surveyed by Perry *et al.* (2013), 21% were net negative (erosional) and 26% were net positive (accretional). They also identified a live coral cover threshold of 10%; reefs with less than 10% live coral cover were net negative in carbonate production. Additionally, they found that relict *Acropora palmata* reefs were more likely to be net negative than *Montastraea* spur and groove formations. *Montastreaea spp.* have become the dominant reef building species in the Caribbean, a role formerly held by *A. palmata* throughout the Quaternary until approximately the 1980s (Tager *et al.* 2010). Perry *et al.* (2013) have attributed these reductions in carbonate production to ecological declines associated with anthropogenic influences. As of 2013, seven key reef building species in the Caribbean have been proposed for placement under the Endangered Species Act, including *A. palmata, A. cervicornis* and three *Montastraea* species (NOAA 2013).

Therefore, the purpose of this study was to investigate the wave processes and current velocities at a barrier reef and lagoon using tidal range as a proxy for sea level rise. This study seeks to better understand and quantify the potential changes that may be

associated with an increase in sea level from a field-based perspective. It is hypothesized that wave energy reduction and lagoon flushing will decrease with sea level rise and assumes a reef that is net erosional with high tide conditions representative of low tide at a sustained elevated sea level.

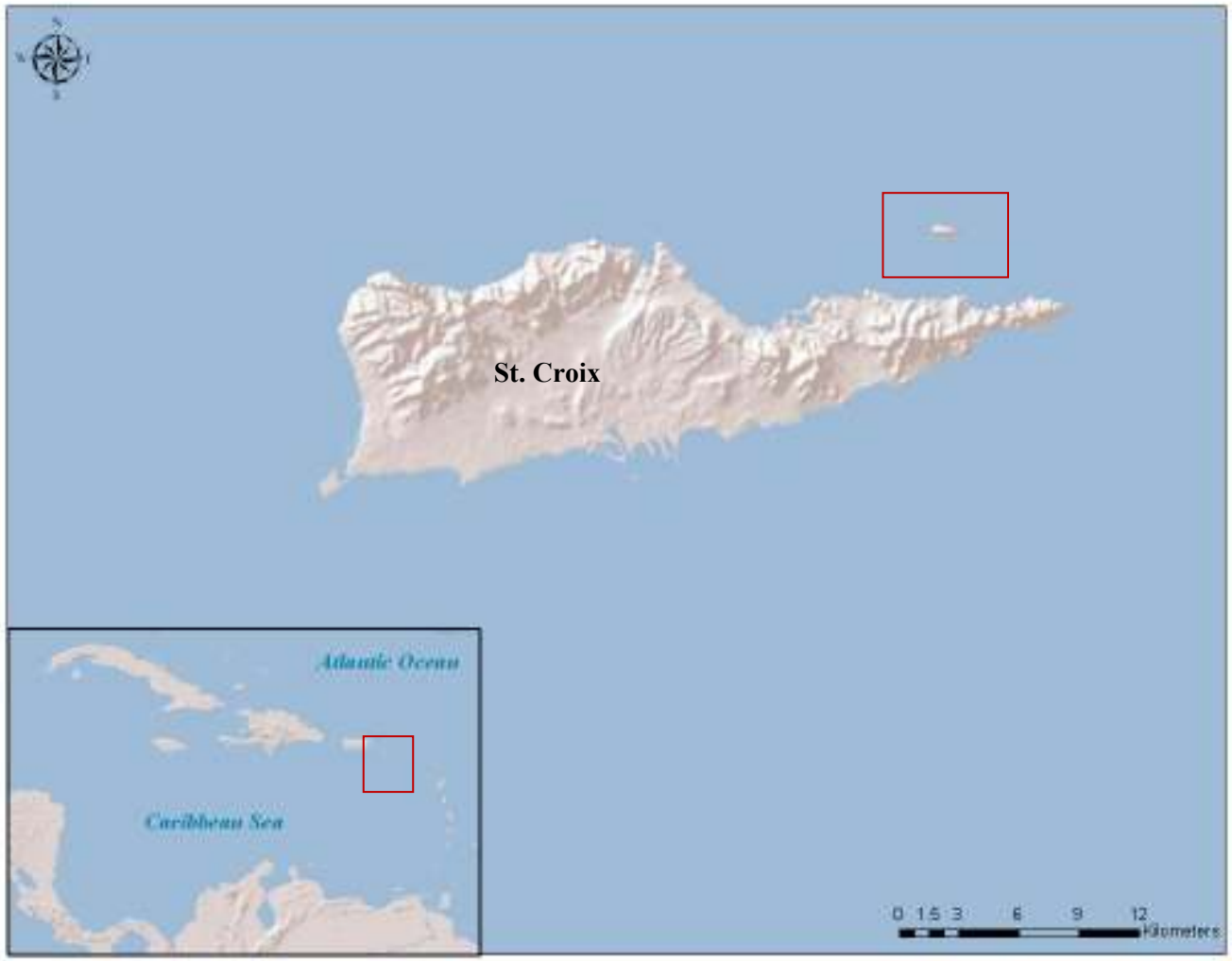

Figure 1. St. Croix is located among the Greater Antilles islands of the Caribbean (inset). Buck Island Reef National Monument is located approximately 2 km northeast of St. Croix. Data provided by ESRI.

CHAPTER 2

METHODS

2.1 STUDY SITE

This study took place at Buck Island Reef National Monument (BIRNM) from 11-18 November 2012. Buck Island is located approximately 2 km northeast of St. Croix in the Caribbean (Fig. 1) and is managed by the National Park Service (NPS). This is a barrier reef system that extends from the southeastern side of the island counter-clockwise to the western side of the island to form Buck Island Bar. The study site was specifically located on the southeast reef (17.78^{o}N 64.61^{o}W) where there is a well-formed lagoon with a cleaner reef profile than the opposing side of the island. BIRNM is a microtidal environment with the predominant winds from the easterly trades (National Park Service, 2011). Meteorological data were collected from a nearby NOAA station "CHSV3" in Christiansted Harbor, 6 km southwest of Buck Island on St. Croix.

Bathymetry data (Fig. 2) was derived from a 2011 LiDAR survey by NOAA's Center for Coastal Monitoring and Assessment (Available from: www.ccma.nos.noaa.gov/ecosystems/coralreef/stcroix_data.aspx) and used to construct benthic habitat maps. The bathymetry indicates the shelf offshore is approximately 12 to 17 meters below sea level (MBSL) rising abruptly to a steep forereef slope with a gradient of 16% and transitioning to a lagoon that ranges from 1 to 4 MBSL. The

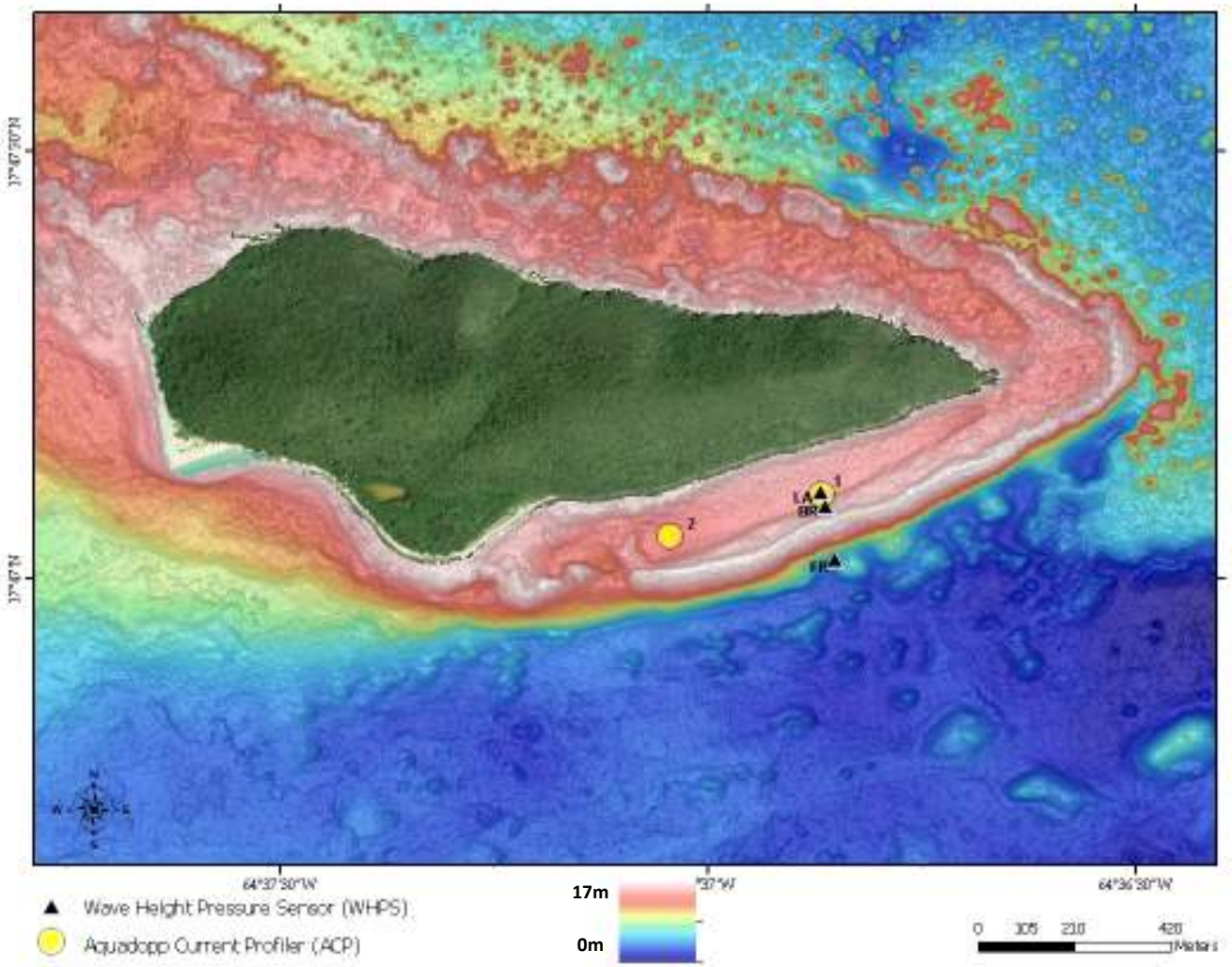

Figure 2. Bathymetry map derived from a 2011 NOAA LiDAR survey.

spatially coincident habitat maps (Fig. 3) show that within the study site, the reef structure is characterized as aggregate reef surrounded by several patch reefs. Visual observations reveal that *Acropora palmata* (Fig. 3A) comprises the aggregate reef and *Montastraea annularis* was the major species comprising the patch reefs (Fig. 3B). According to a 2011 NPS survey, the live coral cover on the south forereef at Buck Island was down to nearly 6% (Fig 4., modified from www.science.nature.nps.gov/im/units/sfcn/coralstatus.cfm), below the 10% live coral threshold (Perry *et al.* 2013).

2.2 FIELD EXPERIMENT

Several instruments were used to quantify the hydrodynamics of this reef system. In order to determine the wave characteristics, three wave height pressure sensors (WHPS), designed and built by the Marine Science Institute at the University of California, Santa Barbara, were deployed in a cross reef transect.. The sensors were secured to cinder blocks, deployed 0.27 m above the bed, and programmed to sample continuously using a 4 Hz sample rate. The WHPS are labeled 'FR' for the forereef location, 'BR' for the back reef location and 'LA' for the lagoon location. FR was deployed in 12.3 m of water 240 from shore, BR in 1.3 m of water and 136 m from shore and LA in 2.4 m of water and 126 m from shore (Fig. 5).

Current velocity and direction data were collected with two 2 MHz Nortek Aquadopp current profilers (ACP) deployed in the lagoon. One of the ACPs, 'ACP1' was co-located with LA while 'ACP2' was located at the opening of the lagoon channel (Fig. 2). The ACPs collected data using 10 minute profiling intervals with an averaging interval of 10 minutes. The bin size, *c*, of the profiler was set to 0.5 m for both locations

with a blanking distance, b, of 0.2 m. The ACPs were bottom mounted to a specialized metal frame 0.13 m above the bed (h_{bed}). All instruments were deployed using rope to enable a guided placement on to sandy substrate.

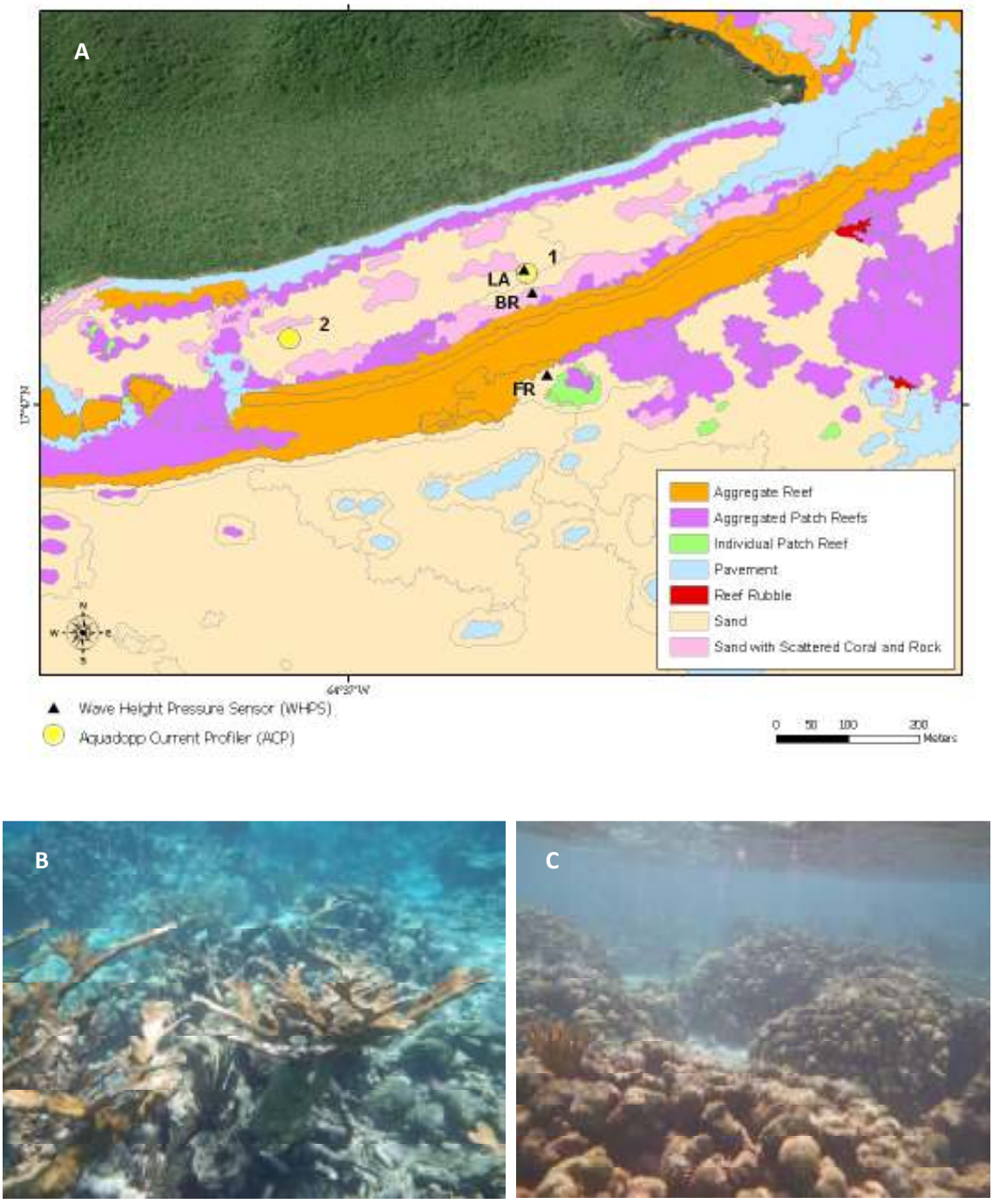

Figure 3. A) Benthic habitat maps derived from a 2011 NOAA LiDAR survey. B) The 'Aggregated Reef' is comprised primarily of *Acropora palmata,* Elkhorn Coral. C) The surrounding 'Aggregated Patch Reefs' are primarily *Montastraea annularis,* Boulder star coral.

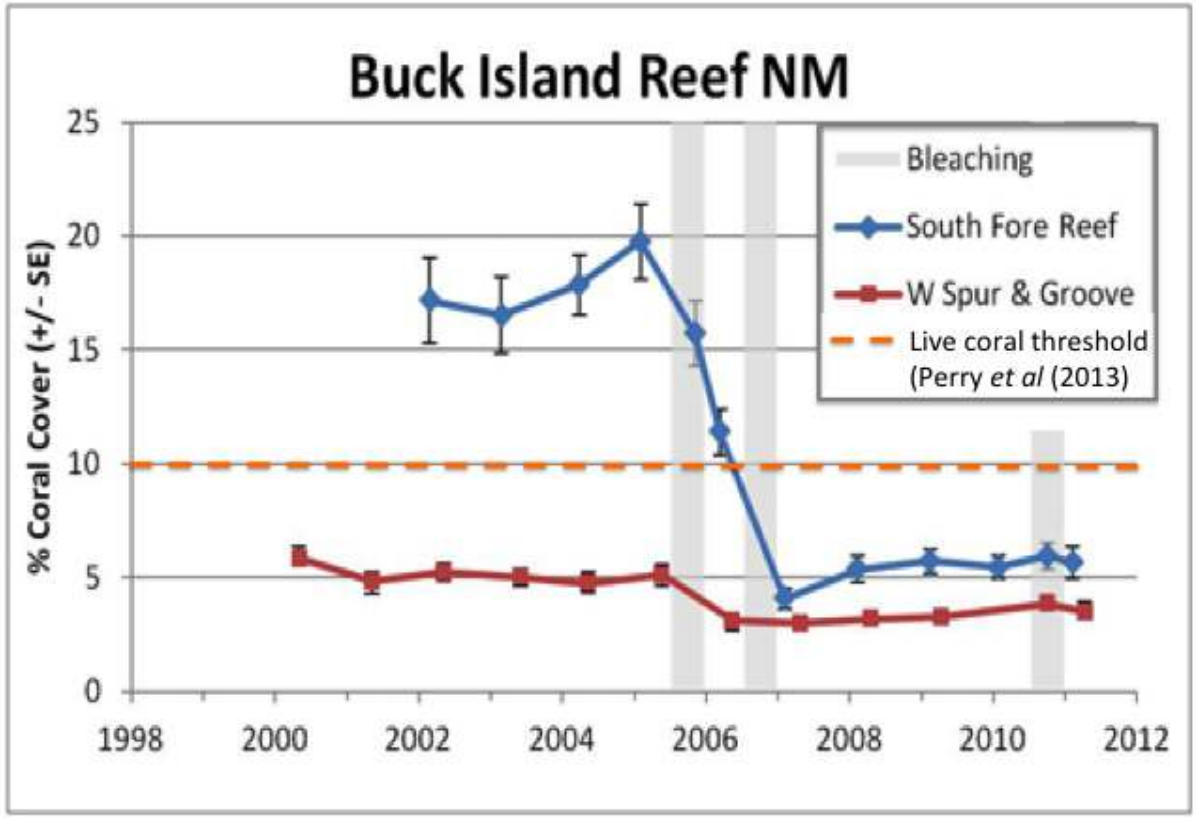

Figure 4. Modified from National Park Service (2011) to display the 10% live coral threshold in the Caribbean identified by Perry *et al.* (2013). Three bleaching events (grey boxes) have been identified as causing a reduction in live coral cover since 2005. The South Fore Reef (location of this study), is below the live coral threshold from 2006-present.

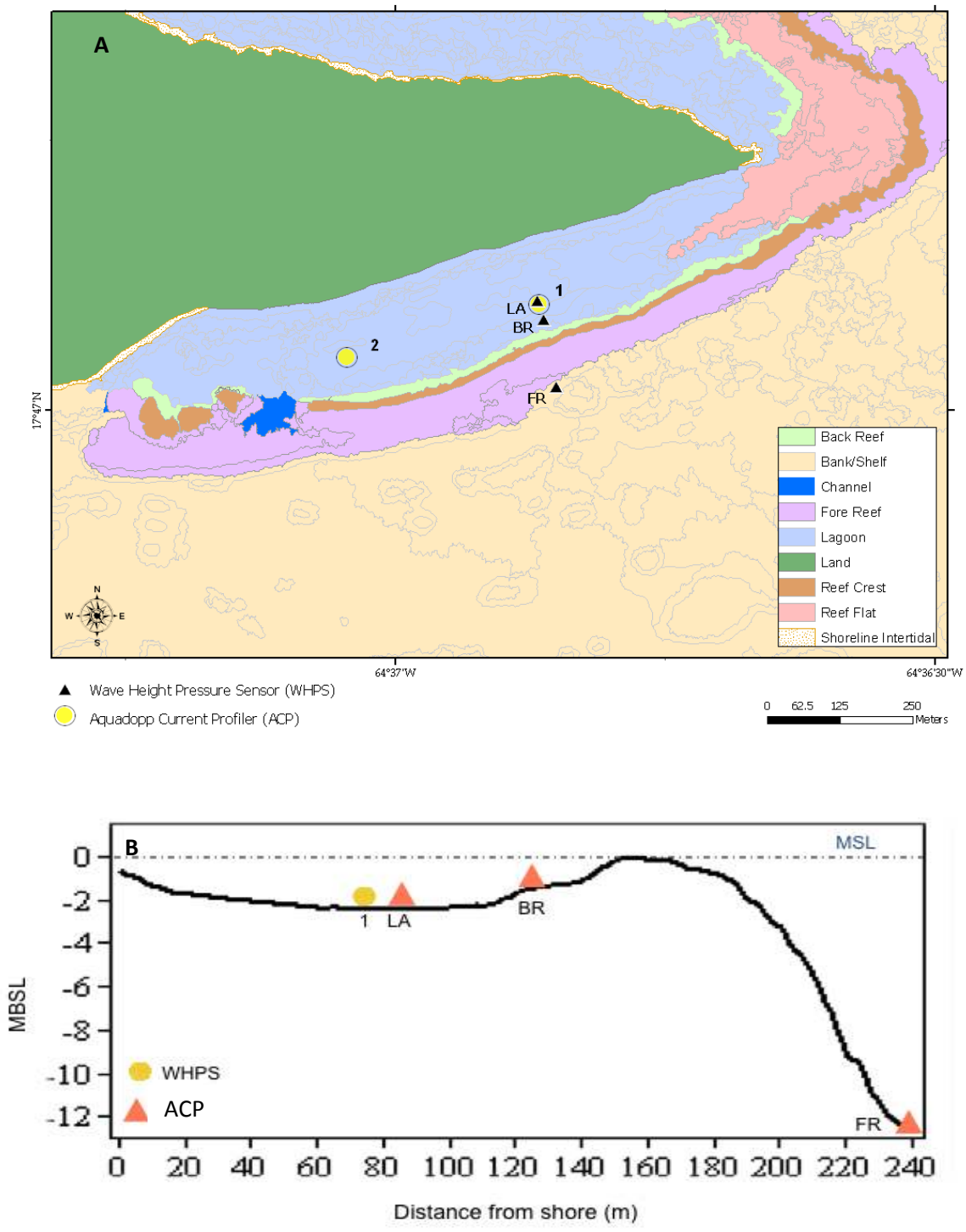

Figure 5. A) The southeast reef complex of Buck Island Reef National Monument. **B)** The reef profile along the instrument transect derived from the LiDAR data with a vertical exaggeration of 10x.

2.3 DATA ANALYSIS

The WHPS were calibrated to convert the instrument output (in counts) to pressure (in dbar) and then converted to sea surface elevation (in meters). Spectral analysis was performed using the Welch method of power spectrum estimation using the Hanning window to determine the dominant wave periods (T_p). The transform length was set to 64 points with an overlap of 0.75 of the transform length for data smoothing. The time series was broken into approximately 17-minute records (4096 samples) and detrended before running a Fast Fourier Transform (FFT) algorithm where a depth attenuation correction was applied. The depth attenuation correction is a high pass filter with cutoff frequencies of 0.25 Hz for the deeper FR location and 0.5 Hz for the shallower BR and LA locations. Next, the inverse of the FFT was determined to estimate significant wave heights (H_s):

$$H_s = 4\sqrt{var(w)} \tag{1}$$

where w is the reconstructed sea surface data. According to Emery and Thompson (2001), it is more efficient to compute the spectrum using FFT as opposed to applying an autocovariance lag window to the time domain.

The WHPS data was used to determine the tidal segments for additional analyses. The observed peaks were identified and plotted alongside data from the NOAA tide gauge in Christiansted Harbor to verify the tidal temporal segments were comparable. A 2.49-hour segment, encompassing six high and seven low tides, was selected to represent 10% of the daily diurnal tidal cycle (Fig. 6).

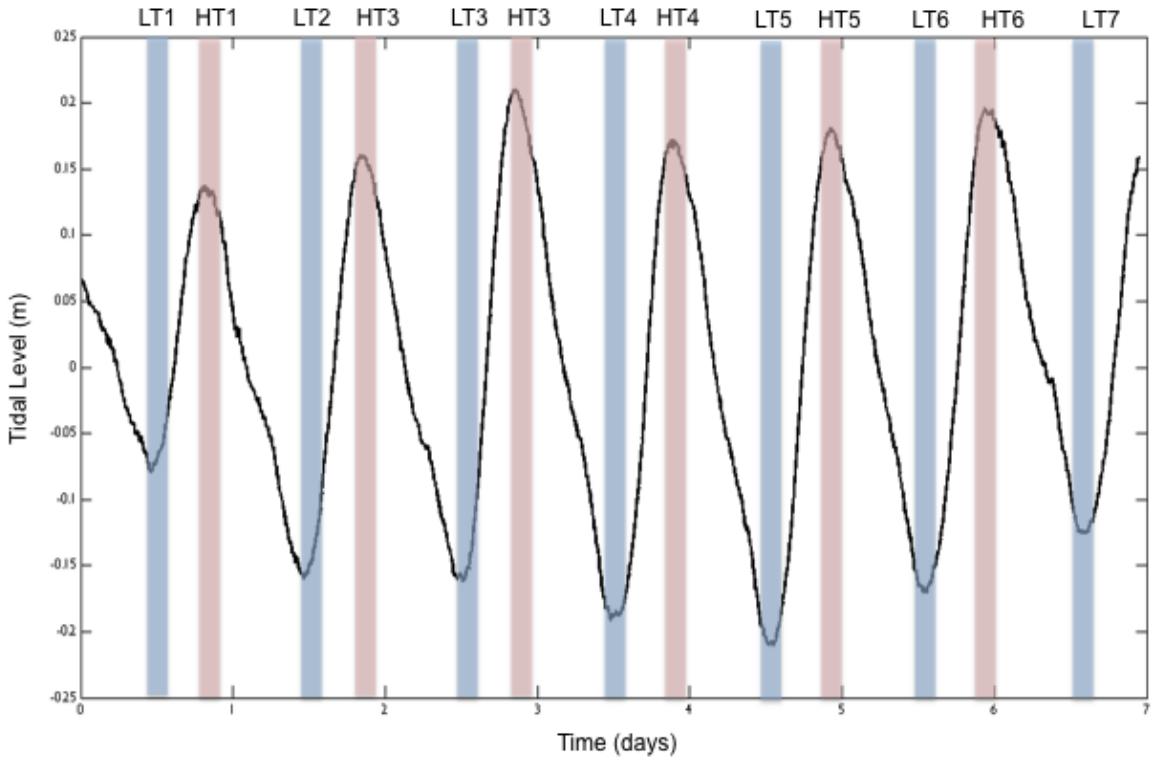

Figure 6. Temporal locations of high and low tide segments identified and labeled. Low tides are displayed in blue and high tides in red.

Using the significant wave heights, wave energy (E) was estimated for each tidal segment:

$$E = \frac{1}{8}\rho g H_s^2 \quad (2)$$

where ρ is the density of seawater (kg m^{-3}), g is the acceleration due to gravity (m s^{-2}) and E is energy (W m^{-2}). The percent energy reduction was determined using:

$$E_{red} = \frac{E_{offshore} - E_{onshore}}{E_{offshore}} x\ 100 \quad (3)$$

from Lugo-Fernandez *et al.* (1998). The 'offshore' and 'onshore' variables change respectively between the different locations being compared, i.e. FR to BR, BR to LA. E_{red} from the FR to BR represents the energy reduction through wave transformation and breaking by the reef. The BR to LA energy reduction was calculated to determine the reduction by continued wave transformation and bottom friction. The energy reduction from FR to LA was calculated to determine the total reduction along the transect.

The bin depth (D) on the ACPs were calculated to determine the usable bins for analysis:

$$D = h_{bed} + b + (i - 1) * c \quad (4)$$

where *i* represents the bin number. Based on these depths, bins 1-3 were used for ACP1 and bins 1-6 for ACP2. The depth-integrated and surface currents were estimated by averaging all usable bins and the upper third of usable bins, respectively.

The currents were rotated in the alongshore (*u*) and cross-shore (*v*) directions. From *u* and *v,* the net current was calculated:

$$\text{Net current} = \sqrt{u^2 + v^2} \quad (5)$$

The temporal durations of the tidal segments were applied to the alongshore, cross-shore and net currents to determine the mean flow velocity and direction (for alongshore and cross shore).

CHAPTER 3

RESULTS

Offshore conditions were collected for the seven-day sampling period (Fig. 7). During this time, the mean wind velocity was 1.74 m s^{-1}, with a mean direction of 107^{o}, or from an ESE direction (Fig. 7a). The tides alternate between mixed semi-diurnal and diurnal, however the tides remained diurnal throughout this study (Fig. 7b). Wave conditions at station 'FR' were used to represent offshore wave conditions. Significant wave heights averaged 0.30 m (Fig. 7c) with dominant wave periods varying between 5-10 s, which is within the range for wind-driven waves (Fig. 7d).

3.1 WAVES

Spectral analysis was run on each of the tidal segments. LT5 and HT4 were selected to depict the spectral characteristics of this sampling period, as the tidal range between these two tides was the greatest and experienced normal offshore forcing conditions i.e. average winds, significant wave heights, and dominant wave periods representative of the seven-day sampling period.

Figure 8 displays the spectral density at the three WHPS locations in the offshore to onshore direction for high tide. The dominant peak observed is in the 0.2-0.1 Hz range,

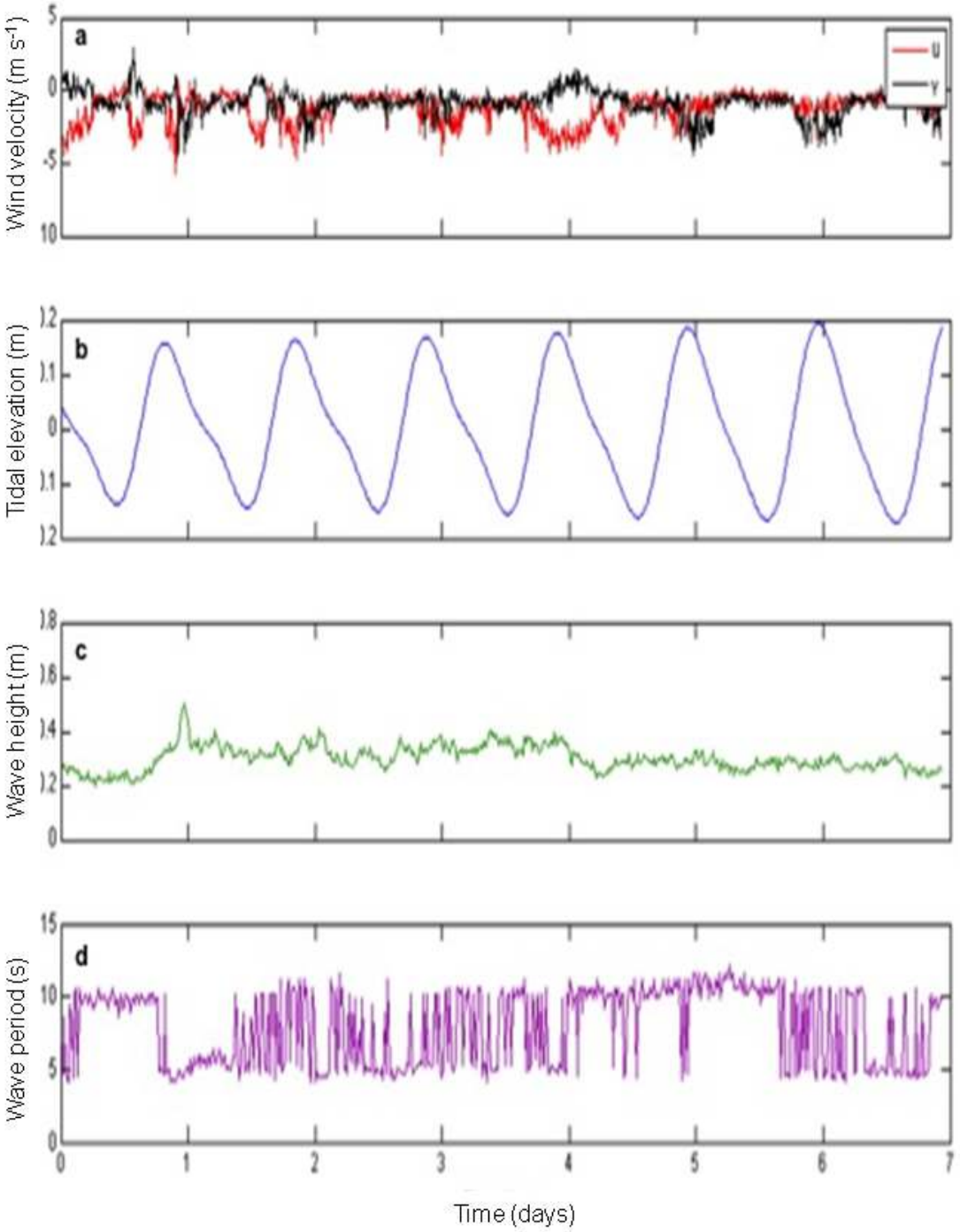

Figure 7. Summary of offshore forcing conditions. **a)** wind velocity collected from NOAA buoy 'CHSV3' at Christiansted Harbor ~6 km SE **b)** tidal levels through the sampling period **c)** significant wave heights collected from FR **d)** dominant wave period collected from FR

representative of wave periods ranging from 5-10 s. This frequency is retained throughout the entire transect and remains as the dominant peak throughout the sampling period. The spectral shape remains relatively uniform for each location suggesting the wave is unbroken as it traverses the reef and propagates into the lagoon.

The spectral density plots for LT5 (Fig. 9) also show dominant peaks in the 5-10 s range. The 10 s peak is most prominent in the FR location. This peak is still observed at BR and becomes less prominent at LA. However, another more prominent peak is observed at all three locations in the ~60 s range (~ 0.016 Hz) but is most pronounced at BR and LA.

The significant wave heights for the sampling period are displayed in Figure 10. H_s at FR is representative of offshore conditions with no strong tidal variability, while the H_s at both BR and LA show a strong tidal dependence. The reduction in H_s can be observed in the along-transect direction, with the smallest waves associated with LA. The differences in the conditions at FR and the tidal dependence observed at BR and LA can be attributed to the influence of the reef. H_s peak observed near day 1 was due to a storm event. Correlation analysis between H_s and water depth (Fig. 11) indicates that there was not a significant relationship between H_s and water depth at FR ($R=0.2012$, $p>0.05$) but a significant relationship between the variables at BR ($R=0.9173$, $p<0.001$) and LA ($R=0.9211$, $p<0.001$).

Using H_s, the wave energy was calculated using Eq. 3 and used to determine the percent energy reduction, E_{red} (Fig. 12), for each interval. Overall, E_{red} from the most

offshore sensor (FR) to the most onshore sensor (LA, Fig. 12A), was 96.00 ± 1.55% at low tide and 64.86 ± 9.11% at high tide. This energy reduction is due to the combination of wave breaking, transformation and frictional losses. To determine the reef contribution to energy reduction, i.e. wave breaking, E_{red} between FR and BR (Fig. 12B) was estimated to be 93.49 ± 2.68% at low tide and 66.88 ± 9.80% at high tide. Losses due primarily to friction from bottom roughness and shallower water are observed between BR and LA (Fig. 12C). The reduction at low tide was 38.15 ± 3.57% and 26.48 ± 5.78% at high tide. Overall, approximately 20-30% more energy was able to traverse the reef at high tide, associated with an increase of 0.4 m of sea level. Energy reduction and wave characteristics are summarized for all high tide (Table 1) and low tide (Table 2) segments.

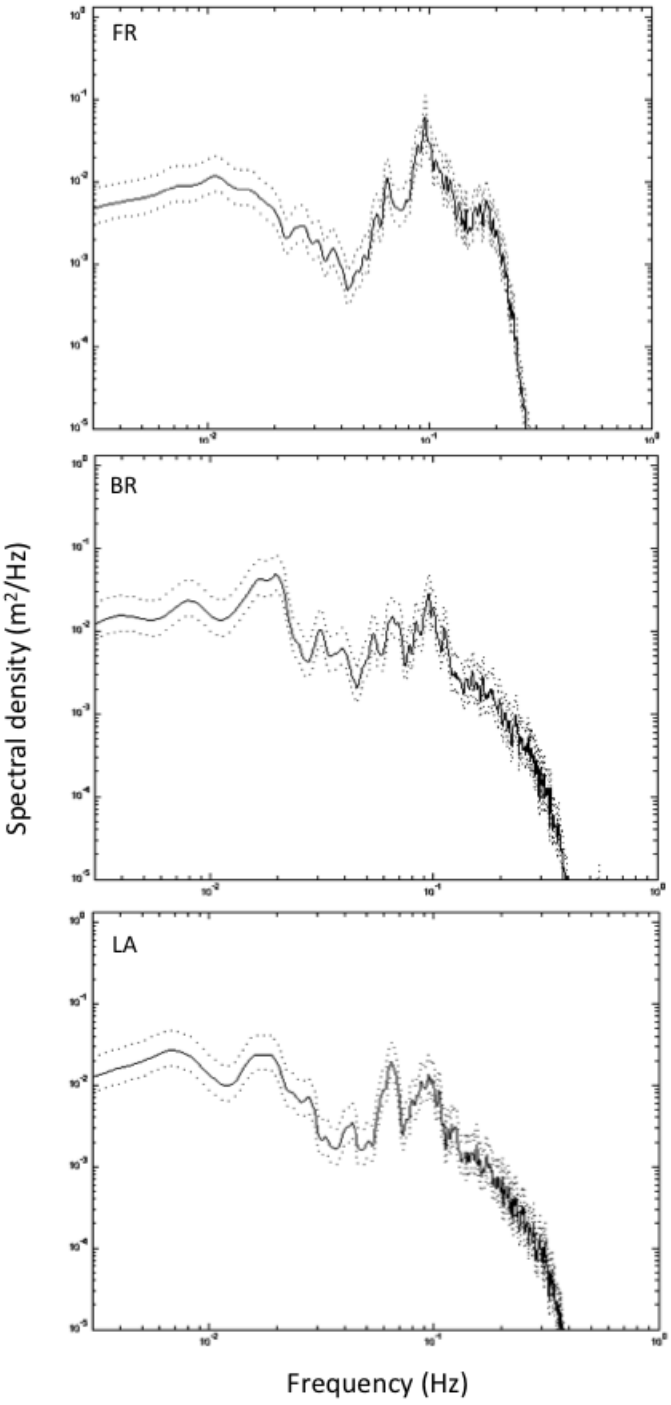

Figure 8. Spectral density plots by location at high tide (HT4).

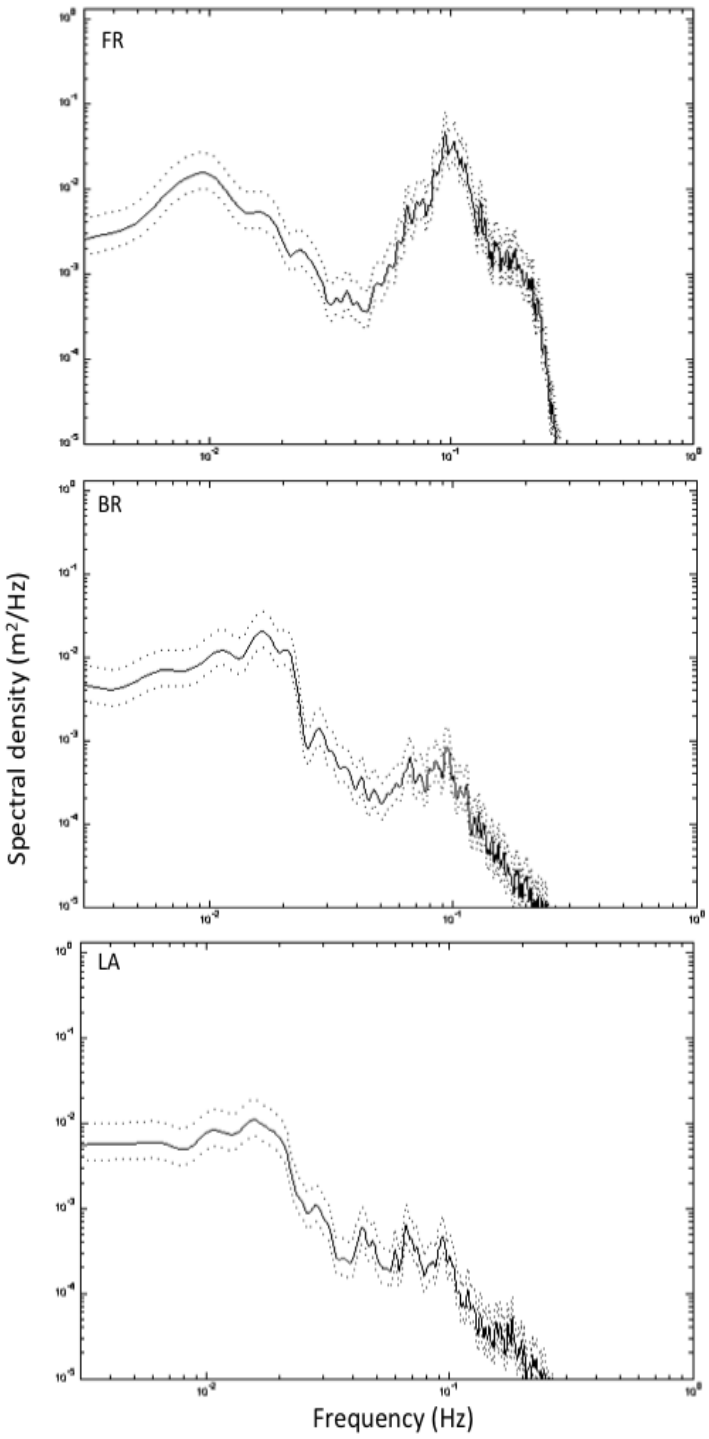

Figure 9. Spectral density by location at low tide (LT5).

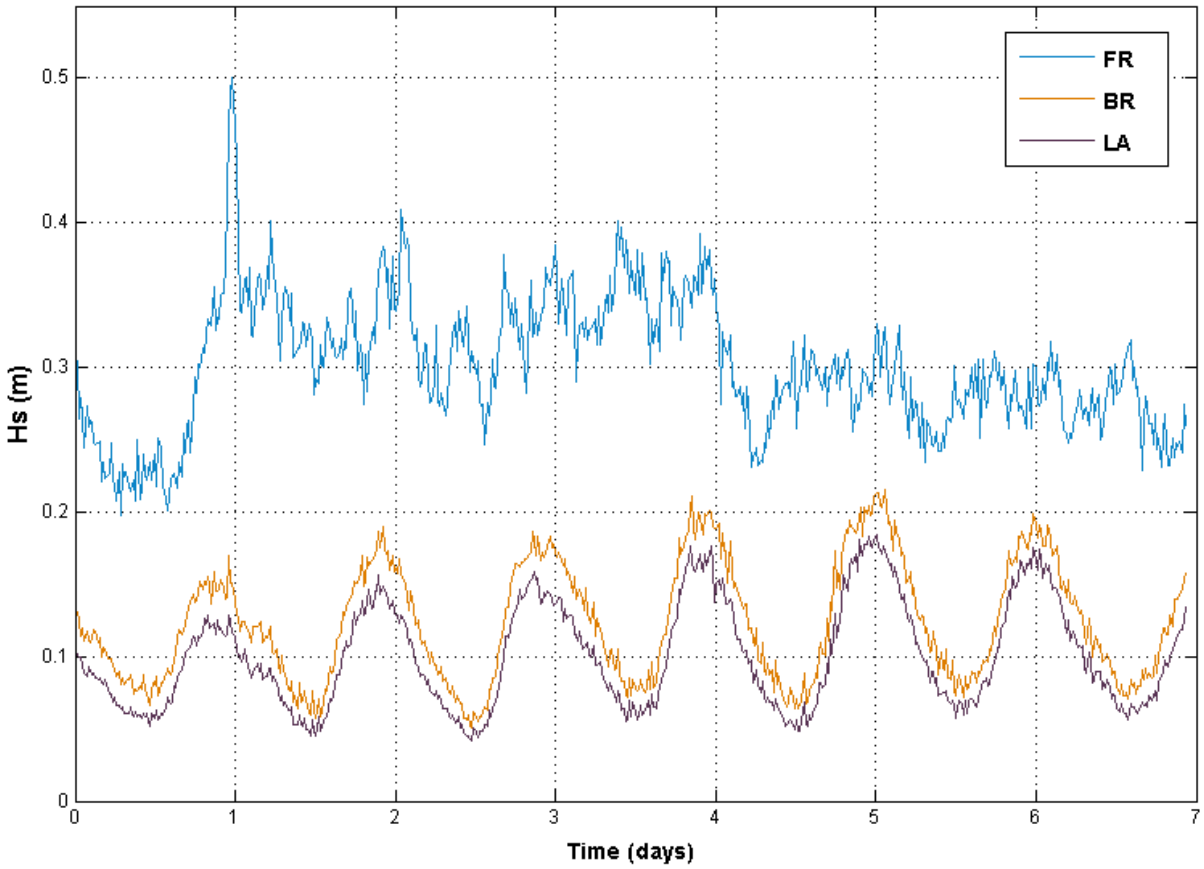

Figure 11. Significant wave height (*H*$_s$) by location. FR is representative of offshore, incident waves. BR and LA display a prominent tidal dependency.

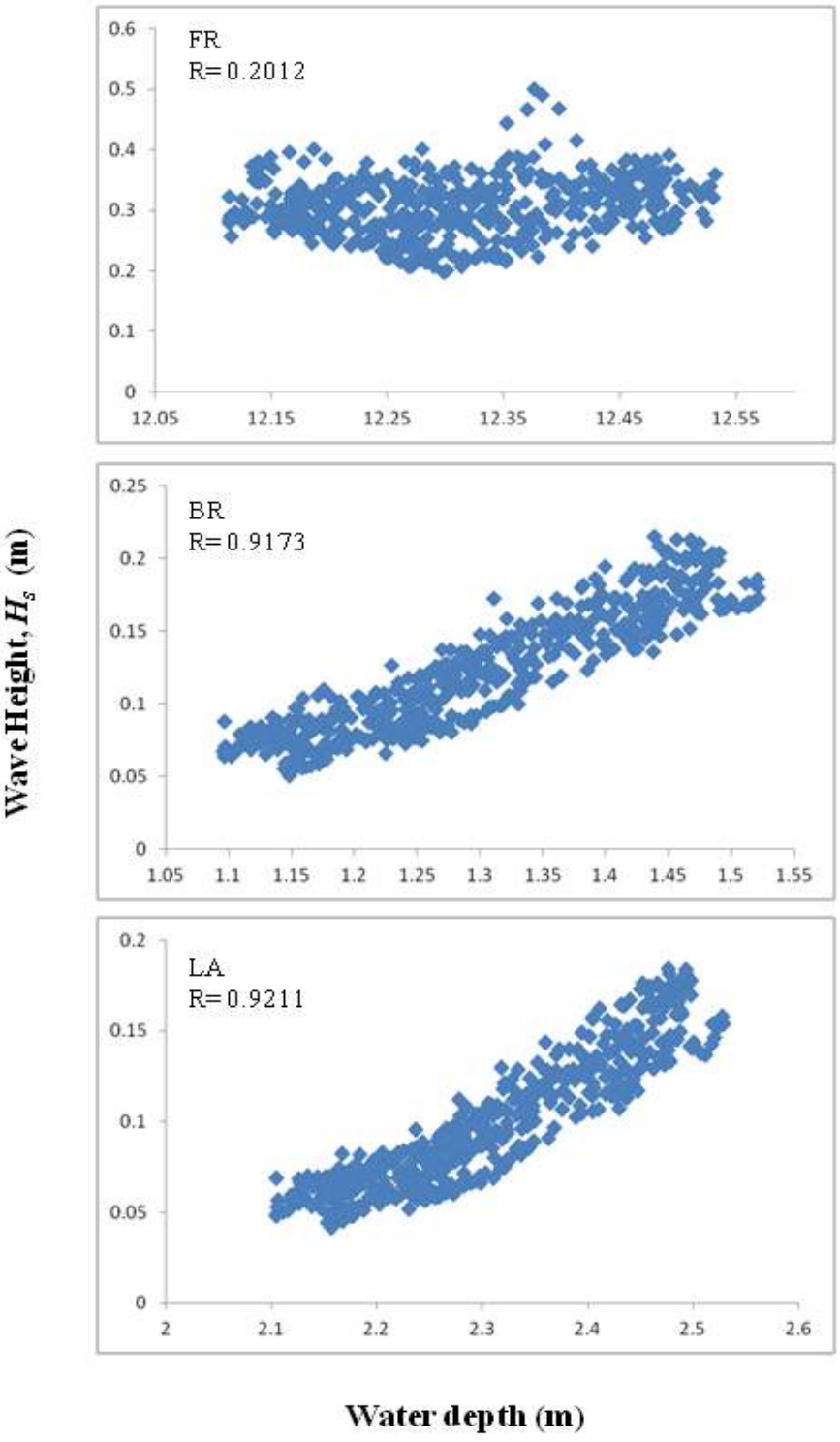

Figure 10. Wave height versus water level by location along the transect with corresponding correlation coefficients.

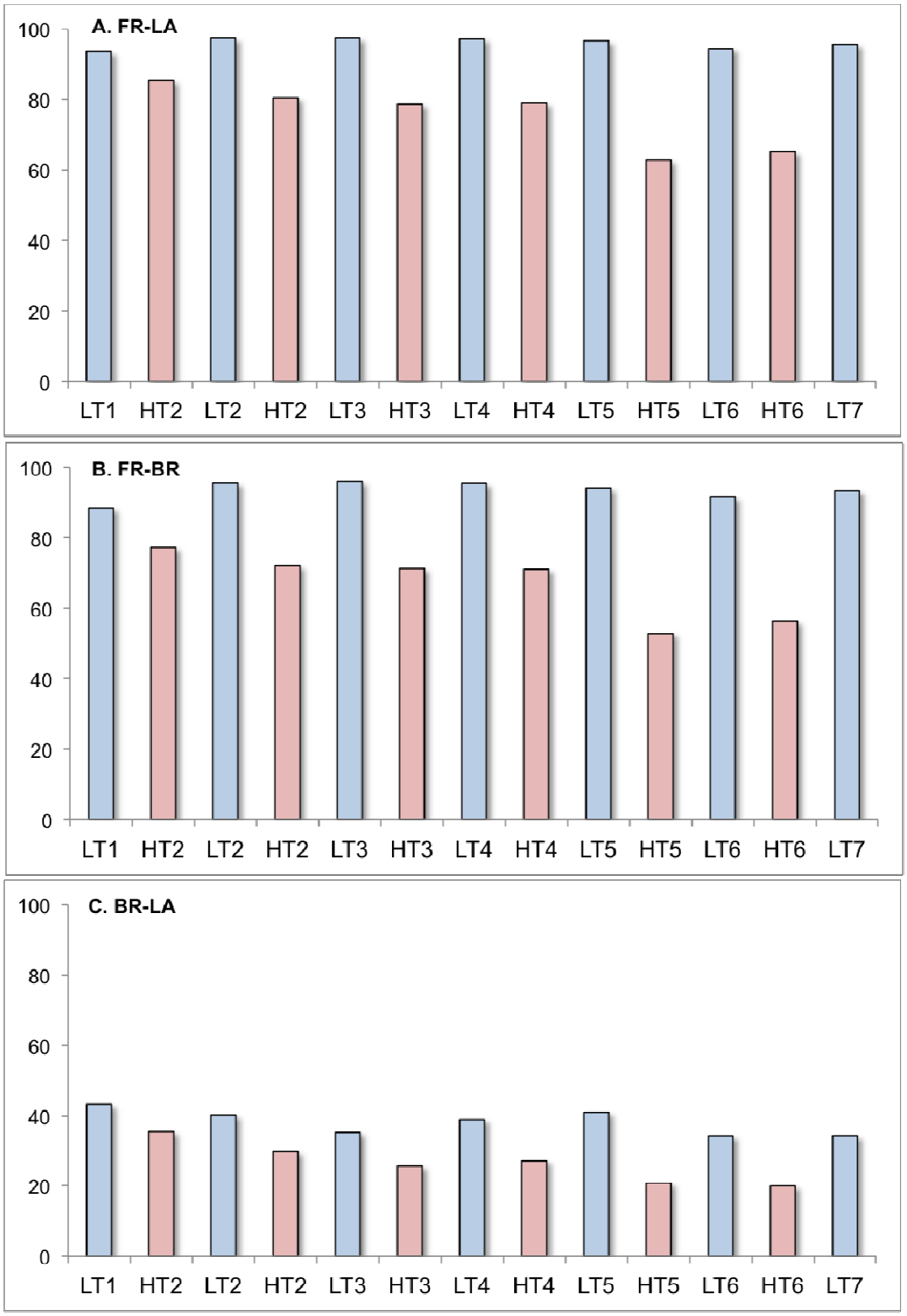

Figure 12. Percent energy reduction determined from $H_{s.}$ **A)** Total E_{red} through the transect **B)** E_{red} from FR-BR, reduction by the reef **C)** E_{red} from BR-LA, reduction due to friction

Table 1. Summary of wave characteristics and energy reduction by high tide segment and location.

Tidal Stage	Location	Tp (s)	Hs (m)	Energy	Reduction	Ered (%)
HT1	FR	6.85	0.3117	1.22E-02	FR-BR	77.33
	BR	10.12	0.1484	2.77E-03	BR-LA	35.48
	LA	10.42	0.1192	1.79E-03	FR-LA	85.38
HT2	FR	9.59	0.3159	1.25E-02	FR-BR	72.15
	BR	11.28	0.1667	3.49E-03	BR-LA	29.77
	LA	11.40	0.1397	2.45E-03	FR-LA	80.44
HT3	FR	6.28	0.3233	1.31E-02	FR-BR	71.37
	BR	10.72	0.1730	3.76E-03	BR-LA	25.62
	LA	10.94	0.1492	2.80E-03	FR-LA	78.70
HT4	FR	5.62	0.3615	1.64E-02	FR-BR	71.14
	BR	57.39	0.1942	4.74E-03	BR-LA	27.20
	LA	22.18	0.1657	3.45E-03	FR-LA	78.99
HT5	FR	8.95	0.2843	1.02E-02	FR-BR	52.95
	BR	58.34	0.1950	4.78E-03	BR-LA	20.84
	LA	39.32	0.1735	3.78E-03	FR-LA	62.76
HT6	FR	8.12	0.2785	9.75E-03	FR-BR	56.35
	BR	37.51	0.1840	4.26E-03	BR-LA	19.98
	LA	15.62	0.1646	3.41E-03	FR-LA	65.07
HTall	FR	7.57	0.3125	1.24E-02	FR-BR	66.88 ± 9.80
	BR	30.89	0.1769	3.97E-03	BR-LA	26.48 ± 5.78
	LA	18.31	0.1520	2.95E-03	FR-LA	64.86 ± 9.11

Table 2. Summary of wave characteristics and energy reduction by low tide segment and location.

Tidal Stage	Location	Tp (s)	Hs (m)	Energy	Reduction	Ered (%)
LT1	FR	9.69	0.2291	6.60E-03	FR-BR	88.53
	BR	52.18	0.0776	7.57E-04	BR-LA	43.17
	LA	60.76	0.0585	4.30E-04	FR-LA	93.48
LT2	FR	6.14	0.3128	1.23E-02	FR-BR	95.52
	BR	66.13	0.0662	5.51E-04	BR-LA	40.18
	LA	78.93	0.0512	3.29E-04	FR-LA	97.32
LT3	FR	5.63	0.2905	1.06E-02	FR-BR	95.96
	BR	70.40	0.0584	4.29E-04	BR-LA	35.23
	LA	81.07	0.0470	2.78E-04	FR-LA	97.38
LT4	FR	8.64	0.3665	1.69E-02	FR-BR	95.45
	BR	70.40	0.0782	7.69E-04	BR-LA	38.95
	LA	77.65	0.0611	4.69E-04	FR-LA	97.22
LT5	FR	9.66	0.2924	1.07E-02	FR-BR	94.14
	BR	66.13	0.0708	6.30E-04	BR-LA	40.96
	LA	76.80	0.0544	3.72E-04	FR-LA	96.54
LT6	FR	10.47	0.2793	9.80E-03	FR-BR	91.51
	BR	66.13	0.0814	8.33E-04	BR-LA	34.26
	LA	81.07	0.0660	5.48E-04	FR-LA	94.42
LT7	FR	5.79	0.2993	1.13E-02	FR-BR	93.36
	BR	69.12	0.0771	7.47E-04	BR-LA	34.29
	LA	54.53	0.0625	4.91E-04	FR-LA	95.64
LTall	FR	8.00	0.2957	1.12E-02	FR-BR	93.49 ± 2.68
	BR	65.79	0.0728	6.74E-04	BR-LA	38.15± 3.57
	LA	72.97	0.0572	4.17E-04	FR-LA	96.00 ± 1.55

3.3 CURRENTS

The top one-third of the depth profile was used to investigate the near surface flow characteristics (Fig. 13). This resulted in the use of one 0.5 m bin for ACP1 and two 0.5 m bins for ACP2. The surface currents were rotated in the alongshore and cross-shore directions for ACP1 and ACP2, shown in Fig. 13A and Fig. 13B, respectively. There was no correlation between the alongshore and cross-shore winds and currents (r^2=0.143 and r^2=0.0024, respectively). The surface currents by tidal segment are summarized in Table 3. For both locations the dominant flow was onshore and westward or towards the lagoon channel opening (Fig. 13C). The cross-shore flow in ACP2 had a strong diurnal signal, which suggests a tidal influence and potentially lagoonal flushing. The depth-integrated alongshore, cross-shore and net currents are displayed in Table 4. The depth-integrated net currents show the flow is higher at ACP2 (Fig. 14). This may be due in part to the larger depth at ACP2 and the interaction with the offshore flow and the proximity to the lagoon channel.

The diurnal signal observed in ACP2 was plotted with the tidal level to determine how the tides influenced these changes in velocities (Fig. 15). This demonstrates that stronger velocities were associated with low tides and slower velocities with high tides (r^2=0.6287, $p<0.01$). Other reef studies (Roberts and Suhayda 1983; Lugo-Fernandez *et al* 1998) observed the same relationship and attributed it to the transfer of breaking wave energy to the current, which is a plausible explanation for this study. Visual observations confirm that wave breaking was minimal at high tide.

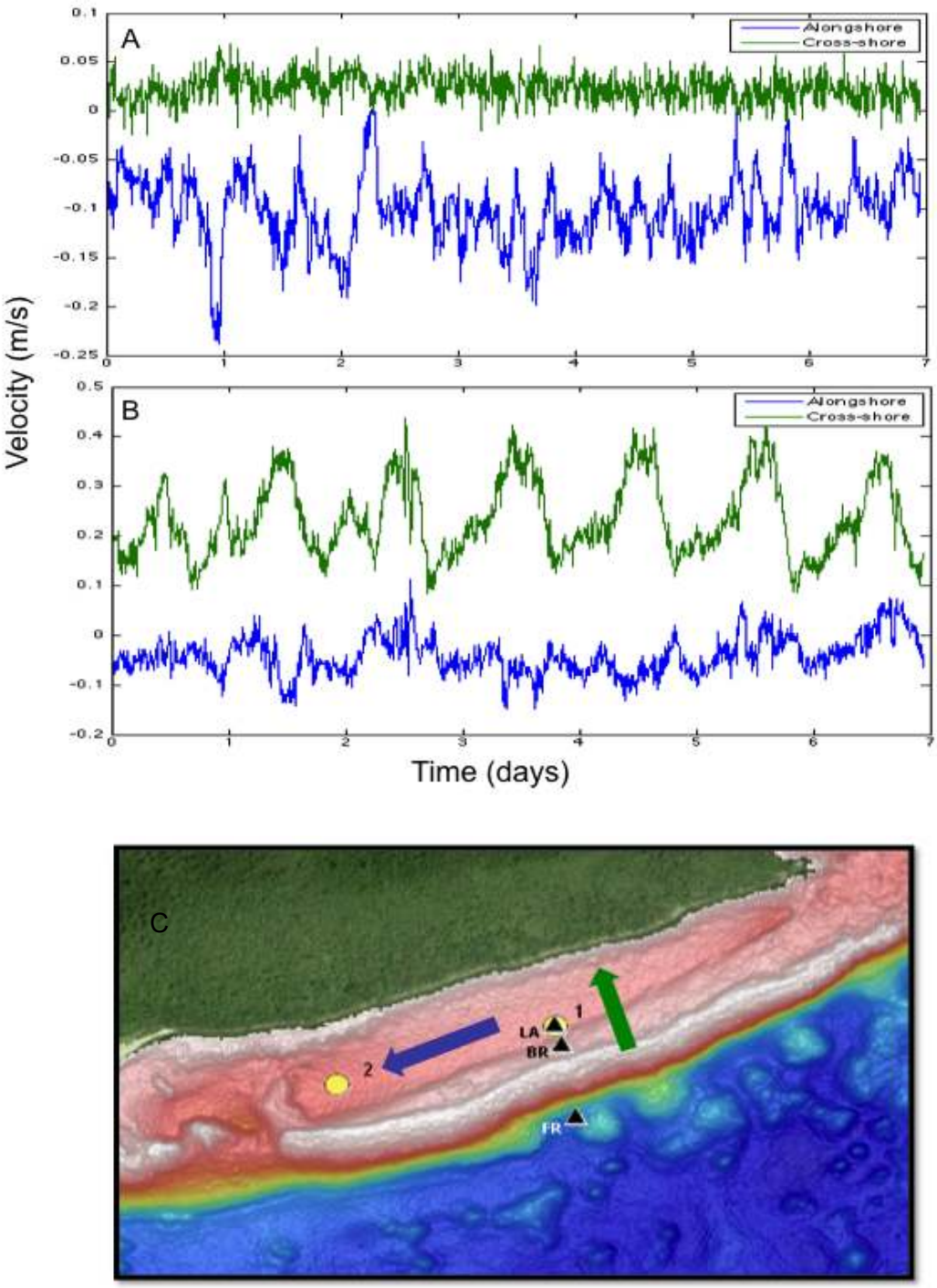

Figure 13. Surface currents from the upper 1/3 of the depth profiles, rotated in the alongshore and cross-shore directions. **A)** ACP1 **B)** ACP2 **C)** The direction of alongshore and cross-shore flows

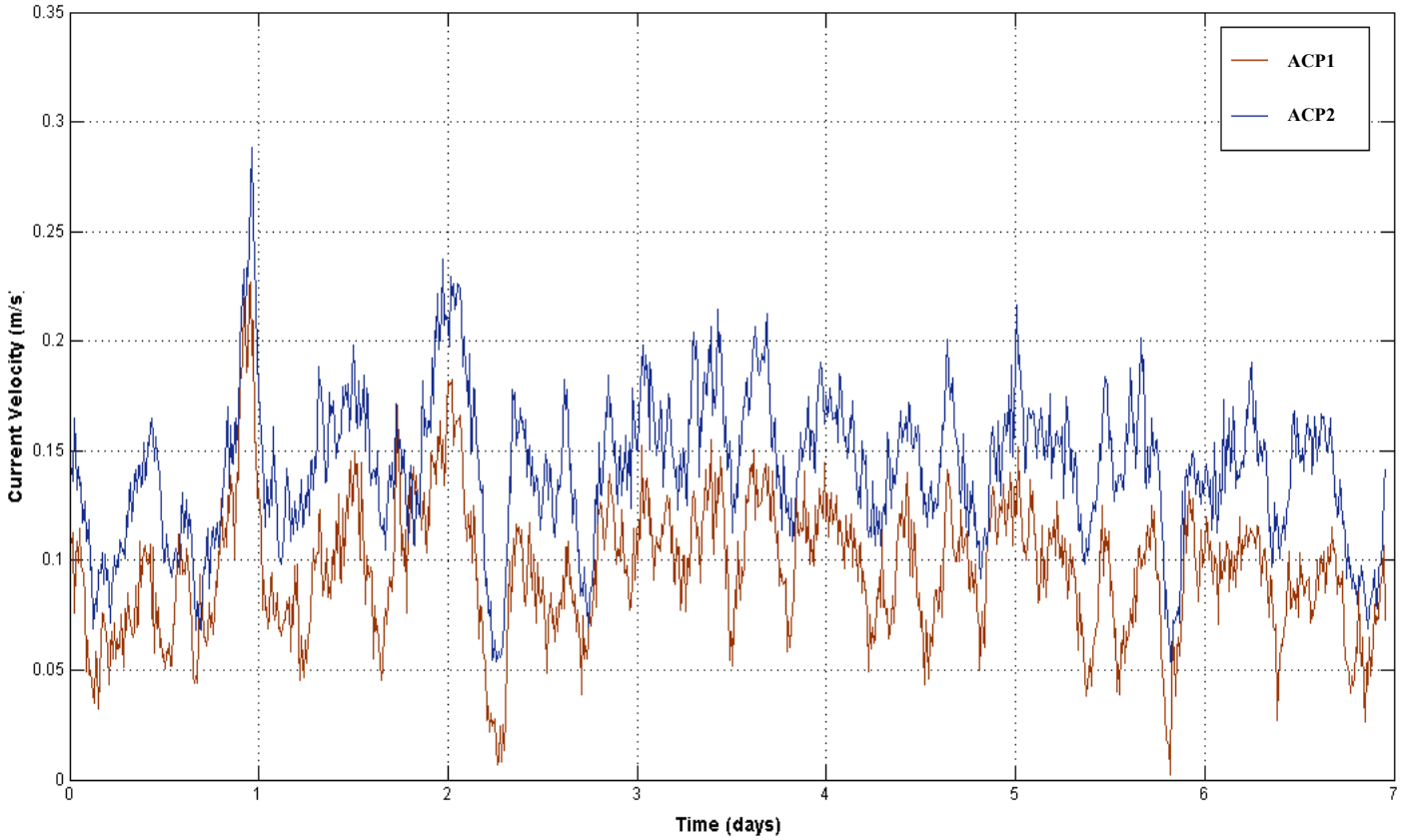

Figure 14. Net currents by location. ACP1 is displayed in red, ACP2 is displayed in blue.

Table 3. Summary of surface currents (top 1/3 of profiles). Bin 3 for ACP1, Bins 5-6 for ACP2

ACP1

Net

LT	(cm/s)	HT	(cm/s)
1	8.50	1	11.51
2	14.24	2	13.29
3	10.05	3	12.67
4	10.77	4	12.44
5	9.18	5	13.38
6	7.33	6	11.05
7	9.98	-	
average:	10.01		12.39
std:	2.18		0.94

Alongshore

LT	(cm/s)	HT	(cm/s)
1	-8.17	1	-10.49
2	-12.35	2	-12.25
3	-7.73	3	-11.68
4	-8.70	4	-11.02
5	-6.79	5	-12.03
6	-6.26	6	-10.60
7	-8.66	-	
average:	-8.38		-11.35
std:	1.98		0.75

Cross-shore

LT	(cm/s)	HT	(cm/s)
1	1.27	1	2.39
2	1.53	2	2.60
3	0.77	3	2.43
4	1.45	4	2.45
5	1.00	5	1.90
6	1.19	6	1.92
7	1.47	-	
average:	1.24		2.28
std:	0.28		0.30

ACP2

Net

LT	(cm/s)	HT	(cm/s)
1	29.97	1	16.22
2	36.86	2	17.05
3	32.93	3	17.21
4	35.40	4	17.77
5	37.49	5	18.25
6	35.69	6	15.63
7	34.79	-	
average:	34.73		17.02
std:	2.56		0.97

Alongshore

LT	(cm/s)	HT	(cm/s)
1	-3.01	1	-4.19
2	-11.21	2	-6.38
3	-0.13	3	-6.61
4	-6.93	4	-5.28
5	-7.88	5	-6.20
6	-0.80	6	-5.97
7	-3.60	-	
average:	-4.79		-5.77
std:	4.03		0.90

Cross-shore

LT	(cm/s)	HT	(cm/s)
1	29.75	1	15.58
2	35.07	2	15.75
3	32.69	3	15.83
4	34.66	4	16.89
5	36.61	5	17.12
6	35.52	6	14.38
7	34.51	-	
average:	34.12		15.93
std:	2.26		0.99

Table 4. Summary of depth-integrated currents, average of bins 1-3 for ACP1 and bins 1-6 for ACP2.

ACP1

Net

LT	(cm/s)	HT	(cm/s)
1	8.3	1	10.79
2	12.46	2	12.54
3	7.84	3	11.96
4	8.89	4	11.31
5	6.93	5	12.22
6	6.43	6	10.79
7	8.82	-	
average:	8.52		11.60
std:	1.96		0.75

Alongshore

LT	(cm/s)	HT	(cm/s)
1	-8.17	1	-10.49
2	-12.35	2	-12.25
3	-7.73	3	-11.68
4	-8.7	4	-11.02
5	-6.79	5	-12.03
6	-6.26	6	-10.6
7	-8.66	-	
average:	-8.38		-11.35
std:	1.98		0.75

Cross-shore

LT	(cm/s)	HT	(cm/s)
1	1.27	1	2.39
2	1.53	2	2.6
3	0.77	3	2.43
4	1.45	4	2.45
5	1	5	1.9
6	1.19	6	1.92
7	1.47	-	
average:	1.24		2.28
std:	0.28		0.30

ACP2

Net

LT	(cm/s)	HT	(cm/s)
1	14.62	1	13.15
2	17.17	2	13.73
3	13.25	3	15.22
4	14.38	4	15.09
5	13.38	5	15.34
6	14.34	6	13.83
7	15.7	-	
average:	14.69		14.39
std:	1.37		0.93

Alongshore

LT	(cm/s)	HT	(cm/s)
1	-4.38	1	-4.52
2	-5.74	2	-5.22
3	-2.97	3	-5.88
4	-3.75	4	-5.29
5	-3.88	5	-6.12
6	-3.33	6	-5.31
7	-3.55	-	
average:	-3.94		-5.39
std:	0.91		0.56

Cross-shore

LT	(cm/s)	HT	(cm/s)
1	13.93	1	12.32
2	16.17	2	12.66
3	12.88	3	14.02
4	13.86	4	14.12
5	12.79	5	14.06
6	13.93	6	12.75
7	15.28	-	
average:	14.12		13.32
std:	1.22		0.83

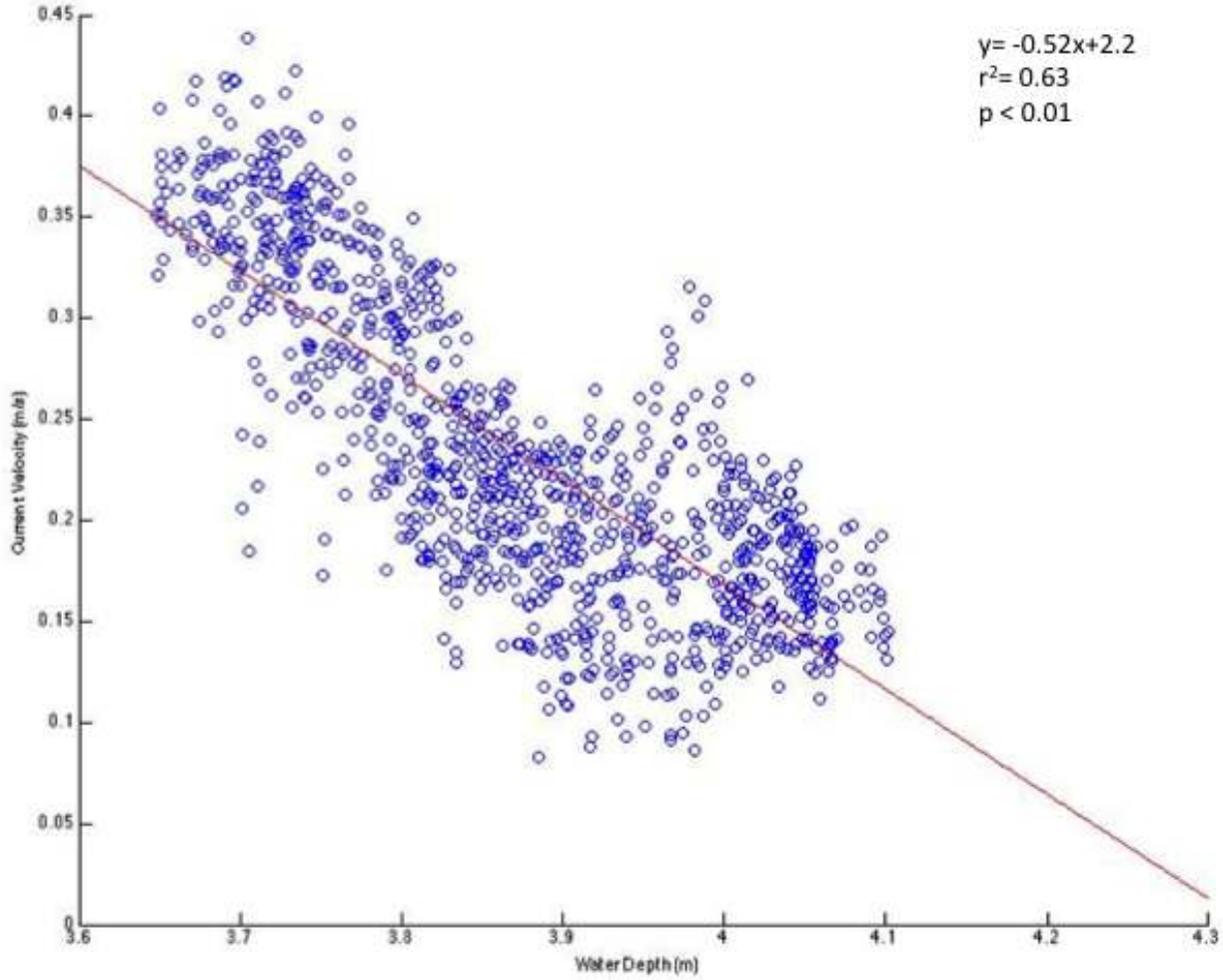

Figure 15. Net surface current from ACP2 with tidal levels. Stronger flows are associated with low tides.

CHAPTER 4

DISCUSSION

This study used tidal range as a proxy for sea level rise and examined variations in hydrodynamics to assess the potential effects of sea level on reef systems. Although reefs have been subject to tidal fluctuations, this study uses high tide conditions to represent a future low tide scenario, with present day maximums becoming future minimums (future low tide). This implies that future high tide conditions would be values higher than observed at any level in this study. The current state of the reef at the Buck Island study site is poor. A bleaching threshold has been crossed on three occasions since 2005, decimating the live coral cover from its previous level of 20% to 6% (Fig 4). A minimum live coral cover of 10% is necessary to maintain a net positive budget in carbonate production and relict *A. palmata* reefs, like those at BIRNM, tend to be net erosional or net negative (Perry *et al.* 2013). This was due in part to the finding that *A. palmata* accretion rates are about 65-70% lower than average Holocene rates. According to these parameters, Buck Island would be classified as a net erosional reef. Since carbonate production is necessary to maintain vertical growth, it is likely that this reef will not be able to accrete at an equivalent rate to sea level rise. Consequently, understanding the potential impact of sea level rise at this location is vital.

4.1 THE IMPACT OF WAVES

The lower frequencies observed typically represent swell or infragravity waves which have been observed in other reef systems (e.g., Pequignet *et al.* 2011, Huang *et al.* 2012, Van Dongeren *et al.* 2013). Van Dongeren *et al.* (2013) modeled infragravity waves at a fringing reef and determined that they are generated within the surf zone and are not due to offshore forcing mechanisms. These infragravity waves were shown to have significant impacts on the bed shear stresses in the lagoon and sediment transport (Su *et al.* 2010, Van Dongeren *et al*. 2013). We observed bed ripples in the lagoon near BR, perhaps suggesting the generation of these infragravity waves. The shoreline of Buck Island is relatively vertical with no dissipative beach. Therefore reflection of waves in the lagoon is probable and is potentially a major contribution to the lower frequencies observed.

The average energy reduction observed during the sampling period is tidally dependent. The average FR to BR reduction is 66.88 ± 9.80 % for high tide and 93.49 ± 2.68% for low tide. With a tidal increase ranging from 0.35-0.5 m from MSL, energy dissipation at the study site decreased by an average of 26% from FR to BR. From FR to LA, energy dissipation decreased by 31%. These data suggest that with an increase of approximately 0.4 m in sea level, a value well within the range of IPCC projected values, that a minimum of 20-30% more energy will traverse the reef crest at low tide. In addition to the 0.4 m sea level rise, this scenario assumes the reef will not vertically accrete, which is likely to occur at BIRNM. As shown in the numerical models by Storlazzi *et al.* (2011), an increase in water depth over the reef decreases the bottom friction, which decreases wave breaking, thus allowing for larger, energetic waves to pass the reef crest. The model also shows that larger wind-waves are able to develop *in situ* on

the reef flat. More energy at the shoreline implies an increase in sediment transport or shoreline erosion. There is an increase in peak-bed wave-induced shear stresses that allow for the transport of terrestrial material (Storlazzi *et al.* 2011).

Impacts related to increasing energy with increasing sea level extend beyond the reef and lagoon. Shoreline erosion is the most obvious consequence of this increase in energy. At Buck Island Reef National Monument in particular, the position and width of the only two sandy beaches on the island are strongly influenced by hydrodynamics, already shifting seasonally. These beaches serve as critical nesting habitat for endangered Leatherback, Hawksbill and Green sea turtles (National Park Service, 2011b) and are beneficial to the recreation and tourism industry. If the magnitude of erosion is high, other species already threatened face even further challenges. A numerical model by Mandlier and Kench (2012) displayed these geomorphic changes. Their simulations indicate that increasing water depth, or sea level, with changes in wave period may shift coral island positions; this concept may be applied to beaches. Mandlier and Kench (2013) state that this depth dependence of wave processes with the reef causes the location of focal and terminal points to shift to leeward sides of the islands as opposed to the windward sides. This shift allows for sediment accumulation on the leeward side and, if the wave convergence zone is beyond the platform, the island may become geomorphically unstable and succumb to the rising seas.

With the anticipated shifts in wave energy associated with the anticipated sea level rise, there could be a shift in coral community composition with reduced rugosity or geomorphic complexity that provides habitat for other marine species (Woodroffe, 2002), and could decrease the overall biodiversity of a reef. This is due in part to the close

relationship observed between wave energy and coral community structure (Geister 1977; Woodroffe 2002; Tager *et al.* 2010). Coral species are often found to be associated with certain wave energy regimes (Fig 16). Domal or massive corals (*Diploria* and *Montastraea*) are associated with lower energy regimes and branching corals (*A. cervicornis)* in moderate energy environments. As energy increases to higher levels, the dominant species shift to platy branching corals (*A. palmata*) then followed by the "weedy species" (*Millepora*). Very high energy environments shift to coralline algae or encrusting corals that can withstand these harsher environments (Geister 1977, Woodroffe 2002).

4.2 THE IMPACT OF CURRENTS

The current velocities are shown to have noticeable depth dependence in ACP2, which is the deeper profiler situated near the opening of the lagoon. The lack of a depth dependency on current velocities in ACP1 is likely due to the central location within the lagoon and the effects of wave setup (Su *et al.* 2010; Pequignet *et al.* 2011). In earlier studies of these processes (e.g. Suhayda and Roberts 1975; Roberts and Suhayda 1983; Lugo-Fernandez *et al.* 1998) currents were generally higher at low tide and were linked to an increase in wave breaking by the reef with the wave energy being transferred to driving the currents. A more recent study concluded that higher water levels over the reef were associated with a reduction in wave-driven flows, which is similar to the findings of this study (Taebi *et al.* 2011). Conversely, when modeling the impact of +1.0 m of sea level on the currents in a reef system Storlazzi e*t al.* (2011) indicated an increase in water depth would result in stronger currents due to the larger, more energetic waves passing the reef crest. This drives the currents and reduces the roughness, thus allowing for less

resistance and swifter currents. The response of current interactions may be more complex and vary with reef morphology. Both scenarios have implications for sea level rise. With a reduction in current velocities, there would be a reduction in flushing rates of the lagoon (Roberts and Suhayda 1983, Roberts *et al.* 1975, Lugo-Fernandez *et al.* 1998a, Taebi *et al.* 2011). Flushing of the lagoon is important for the moderation of temperature, salinity and water clarity (Roberts *et al.* 1975, Lugo-Fernandez *et al.* 1998, Hearn 1999, Storlazzi *et al.* 2011) and therefore critical for coral health. Taebi e*t al.* (2011) suggested that a moderate sea level increase would lead to a reduction in lagoon flushing.

Within the same context, sediment transport and turbidity would be impacted by these shifts in current velocities. With an increase in current velocities, sediment transport rates may increase on the reef and along the shoreline (Lugo-Fernandez *et al.* 1998,Su *et al.* 2010, Storlazzi *et al.* 2011). The model by Storlazzi *et al.* (2011) indicated that the larger waves will result in a higher resuspension of sediment. This was observed in the field with increased concentrations of suspended sediment, associated with higher sea levels (Storlazzi e*t al.* 2004, Presto *et al.* 2006). Higher suspended concentrations have implications for coral health because it is energetically expensive for coral to expel sediment from their surface and sediment can also cause abrasion and burial (Richmond, 1993). *A. palmata* is a species that tends to be inefficient at sediment removal (NOAA, 2012).

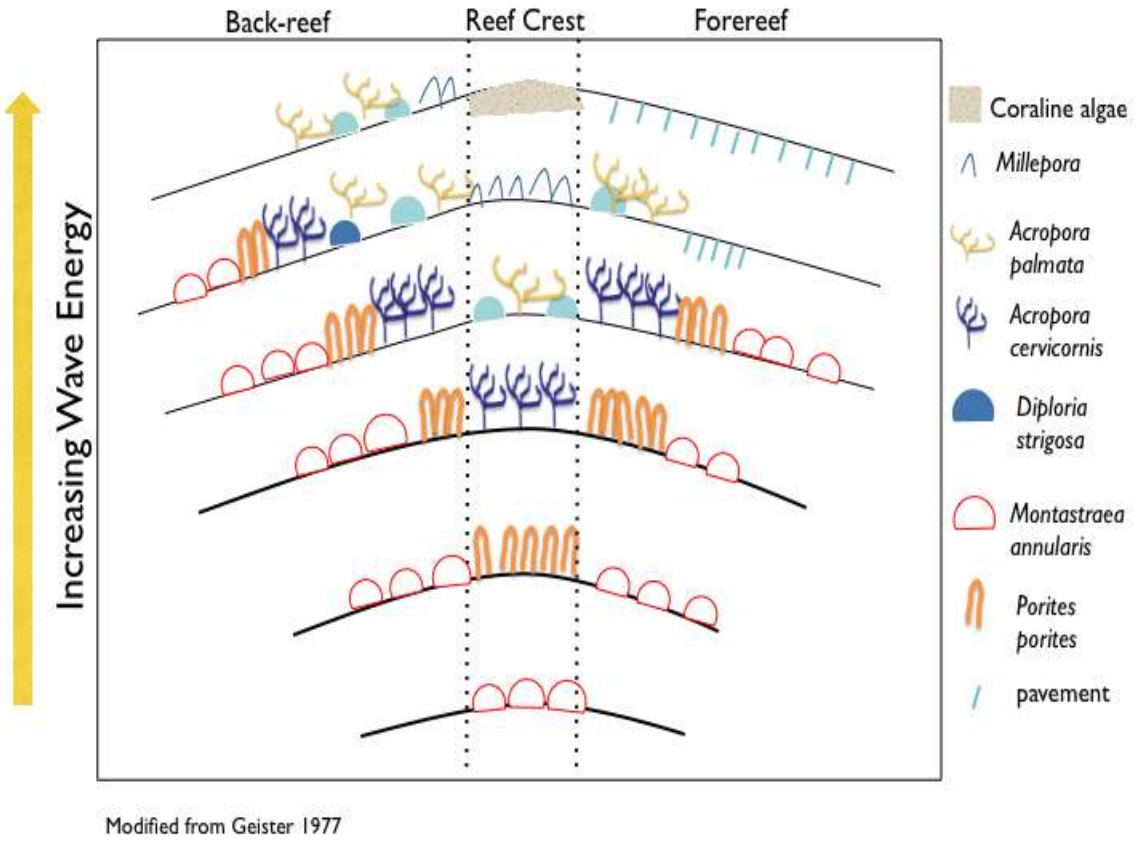

Figure 16. The relationship between wave energy and coral distribution. As wave energy increases, the community composition changes and diversifies until reaching a maximum level where diversity begins to decrease.

4.3 CONCLUSION

With the various environmental factors affecting reef growth, the reef morphology is likely to change and subsequently the impact on the hydrodynamics. The results of this study indicate that if reefs are unable to maintain growth rates equivalent to that of sea level rise, there will be more energy transferred to shore, shifts in flow regimes and changes in coral community structures.

The Buck Island National Monument's General Management Plan (unpublished draft; personal communication, Ian Lundgren), states that there is a serious threat to the Park's natural resources and visitor activities over the long term due to the effects of climate change from sea level rise, loss of critical habitat, loss of coral reefs and fisheries as well as the threats faced by ocean acidification. In an effort to assess how the hydrodynamics of reef systems will be impacted by changes in sea level, this study used tidal range as a proxy for sea level rise and examined variations in wave energy dissipation and current velocities. The chief findings of this study were as follows:

1. Energy reduction is decreased from 20-30% at high tide, approximately 0.4 m higher than low tide. More energy propagates to the shoreline at higher sea level.
2. Current velocities are impacted by wave breaking and will be reduced with higher sea level and a reef lagging in vertical accretion, potentially decreasing lagoonal flushing.
3. The available parameters of successful reef accretion indicate that Buck Island Reef National Monument may not maintain an equal pace with sea level if current conditions persist

REFERENCES

Bythell JC, Gladfelter EH, Gladfelter WB, French KE and Hillis Z (1989) Buck Island Reef National Monument- changes in modern reef community structure since 1976. Terrestrial and Marine Geology of St. Croix, U.S. Virgin Islands: West Indies Laboratory, Special Publication, 8: 145-154.

Davidson-Arnott, R. Introduction to Coastal Processes and Geomorphology (2010) Cambridge University Press, New York. Print.

Ellis JT, Sherman DJ, Bauer BO and Hart J (2002) Assessing the impact of an organic restoration structure on boat wake energy. Journal of Coastal Research, SI36: 256-265.

Hearn CJ (2011) Perspectives in coral reef hydrodynamics. Coral Reefs, 30: 1-9.

Hearn CJ (1999) Wave-breaking hydrodynamics within coral reef systems and the effect of changing relative sea level. Journal Geophysical Research, 104 (C12): 30,007-30,019.

Huang ZC, Lenian L, Melville WK, Middleton JH, Reineman B, Statom N and McCabe RM (2012) Dissipation of wave energy and turbulence in a shallow coral reef lagoon. Journal of Geophysical Research, 117, C03015.

Hubbard DK, Zankl H, Van Heerden I and Gill IP (2005) Holocene reef development along the northeastern St. Croix shelf, Buck Island, U.S. Virgin Islands. Journal of Sedimentary Research, 75 (1): 97-113.

Hubbard DK, Parsons KM, Bythell JC, and Walker ND (1991) The effects of Hurrican Hugo on the reefs and associated environments of St. Croix, U.S. Virgin Islands- a preliminary assessment. Journal of Coastal Research, SI8: 33-48.

Kathiresan K and Rajendran N (2005) Coastal mangrove forests mitigated tsunami. Estuarine Coastal and Shelf Science, 65: 601-606.

Larcombe P, Costen A, Woolfe KJ (2001) The hydrodynamic and sedimentary setting of nearshore coral reefs, central Great Barrier Reef shelf, Australia: Paluma Shoals, a case study. Sedimentology, 48: 811-835.

Lugo-Fernandez A, Roberts HH, and Suhayda JN (1998) Wave transformations across a Caribbean fringing-barrier coral reef. Continental Shelf Research, 18: 1099-1124.

Lugo-Fernandez A, Roberts HH, Wiseman Jr WR, (1998a) Tide effects on wave attenuation and wave set-up on a Caribbean coral reef. Estuarine, Coastal and Shelf Science, 47:385-393.

Madin JS and Connolly SR (2006) Ecological consequences of major hydrodynamic disturbances on coral reefs. Nature, 444: 477-480.

Mandlier PG and Kench PS (2012) Analytical modeling of wave refraction and convergence on coral reef platforms: Implications for island formation and stability. Geomorphology, 159-160: 84-92.

Nash C, Doan V, Kageyama K, Atkinson A, Davis A, Miller J, Patterson J, Patterson M, Ruttenberg B, Waara R, Basch L, Beavers S, Brown E, Brown P, Capone M, Craig P, Jones T and Kudray G (2009) Coral Reefs in U.S. National Parks: A Snapshot of Status and Trends in Eight Parks. Natural Resources Report NPS/NRPC/NRR-2009/091, U.S., Department of the Interior, National Park Service.

Neuman AC and MacIntyre I (1985) Reef response to sea level rise: Keep up, catch up or give up. Proceedings of the 5th International Coral Reef Congress, Tahiti, 3: 105-110.

NOAA (2012) Coral Reef Conservation Program. 23 Sep 2011. 4 Jan 2012 http://www.coralreef.noaa.gov

NOAA (2013) Sea Levels Online. 14 April 2013. http://tidesandcurrents.noaa.gov/sltrends/

Péquignet AC, Becker JM, Merrifield MA and Boc SJ (2011) The dissipation of wind wave energy across a fringing reef at Ipan, Guam. Coral Reefs, 30: 71-82.

Perry CT, Murphy GN, Kench PS, Smithers SG, Edinger EN, Steneck RS and Mumby P (2013) Caribbean-wide decline in carbonate production threatened coral reef growth. Nature Communications, 4:1402.

Presto MK, Ogston AO, Storlazzi CD, and Field, ME (2006) Temporal and spatial variability in the flow and dispersal of suspended-sediment on a fringing reef flat, Molokai, Hawaii. Estuar Coast Shelf Sci, 67: 67-81.

Quartel S, Kroon A, Augustinus PGEF, Van Santen P and Tri NH (2007) Wave attenuation in coastal mangroves in the Red River Delta, Vietnam. Journal of Asian Earth Sciences, 29: 576-584.

Richmond RH (1993) Coral reefs: Present problems and future concerns resulting from anthropogenic disturbance. Amer Zoology, 33: 524-536.

Roberts HH (1980) Physical processes and sediment flux through reef-lagoon systems. Proceedings of the 17th Coastal Engineers Conference, Sydney, Australia, pp. 946—962.

Roberts HH and Suhayda JN (1983) Wave-current interactions on a shallow reef (Nicaragua, Central America). Coral Reefs, 1: 209-214.

Roberts HH, Murray S, and Suhayda JN (1975) Physical processes in a fringing reef system. J of Marine Res, 33:233-260.

Roberts HH, Wilson PA and Lugo-Fernandez A (1992) Biologic and geologic responses to physical processes: examples from modern reef systems of the Caribbean-Atlantic region. Cont Shelf Res, 12(7/8): 809-834.

Storlazzi CD, Elias E, Field ME and Presto MK (2011) Numerical modeling of the impact of sea-level rise on fringing coral reef hydrodynamics and sediment transport. Coral Reefs, 30: 83-96.

Taebi S, Lowe RJ, Pattiaratchi CB, Ivery GN, Symonds G and Brinkman R (2011) Nearshore circulation in a tropical fringing reef system. Journal of Geophysical Research, 116, C02016.

Taebi S, Lowe RJ, Pattiaratchi CB, Ivey GN, Symonds G (2012) A numerical study of the dynamics of the wave-driven circulation within a fringing reef system. Ocean Dynamics, 65: 585-602.

Van Dongeren AP, Lowe R, Pomeroy A, Trang DM, Roelvink D, Symonds G and Ranasinghe R (2013) Modelling infragravity waves and currents across a fringing coral reef. Coastal Engineering, 73: 178-190.

Woodroffe CD (2002) Coasts: Form, process and evolution. Cambridge University Press, Cambridge. Print